AD-A138 714 THE FATIGUE OF POWDER METALLURGY ALLOYS(U) CONNECTICUT 1/1
UNIV STORRS INST OF MATERIALS SCIENCE A J MCEVILY
17 JAN 84 AFOSR-TR-84-0111 AFOSR-81-0046

UNCLASSIFIED F/G 11/6 NL

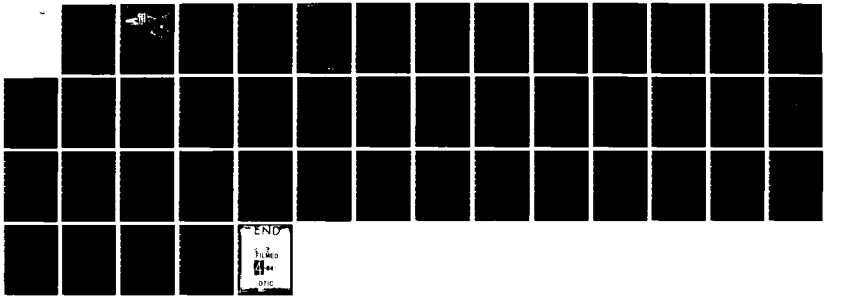

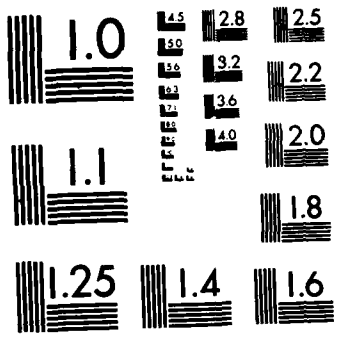

MICROCOPY RESOLUTION TEST CHART
NATIONAL BUREAU OF STANDARDS-1963-A

AFOSR-TR- 84-0111

AD A138714

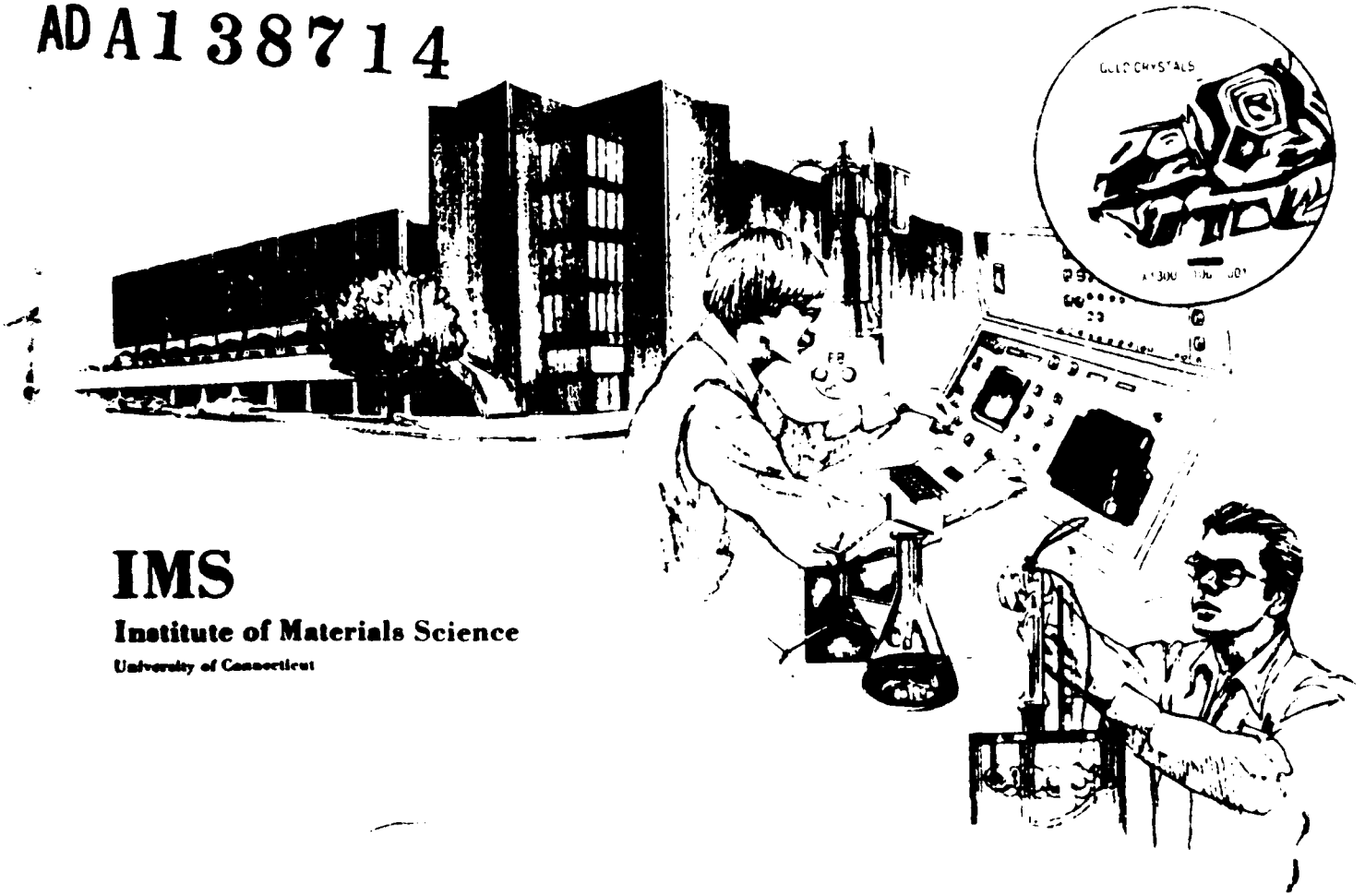

IMS

Institute of Materials Science

University of Connecticut

Annual Report
on
The Fatigue of Powder Metallurgy Alloys
U. S. Air Force Grant No. AFOSR 81-0046

Covering Period
1 December 1982 to 30 November 1983

Submitted by
A. J. McEvily

2

Annual Report
on
The Fatigue of Powder Metallurgy Alloys
U. S. Air Force Grant No. AFOSR 81-0046

Covering Period
1 December 1982 to 30 November 1983

Submitted by
A. J. McEvily

UNCLASSIFIED

SECURITY CLASSIFICATION OF THIS PAGE (When Data Entered)

REPORT DOCUMENTATION PAGE		READ INSTRUCTIONS BEFORE COMPLETING FORM
1. REPORT NUMBER AFOSR-TR- 84-0111	2. GOVT ACCESSION NO. AD-A135714	3. RECIPIENT'S CATALOG NUMBER
4. TITLE (and Subtitle) THE FATIGUE OF POWDER METALLURGY ALLOYS		5. TYPE OF REPORT & PERIOD COVERED Scientific - Annual 12/1/82 - 11/30/83
		6. PERFORMING ORG. REPORT NUMBER
7. AUTHOR(s) A. J. McEvily		8. CONTRACT OR GRANT NUMBER(s) AFOSR-81-0046
9. PERFORMING ORGANIZATION NAME AND ADDRESS University of Connecticut Metallurgy Dept., U-136 Storrs, CT 06268		10. PROGRAM ELEMENT, PROJECT, TASK AREA & WORK UNIT NUMBERS 61102F 2306/A1
11. CONTROLLING OFFICE NAME AND ADDRESS Air Force Office of Scientific Research/NE Bolling AFB, Building 410 Washington, D.C. 20332		12. REPORT DATE Jan. 17, 1984 13. NUMBER OF PAGES 41
14. MONITORING AGENCY NAME & ADDRESS(if different from Controlling Office)		15. SECURITY CLASS. (of this report) Unclassified 15a. DECLASSIFICATION/DOWNGRADING SCHEDULE

16. DISTRIBUTION STATEMENT (of this Report)

This document has been approved for public release, its distribution is unlimited.

17. DISTRIBUTION STATEMENT (of the abstract entered in Block 20, if different from Report)

18. SUPPLEMENTARY NOTES

19. KEY WORDS (Continue on reverse side if necessary and identify by block number)

High Strength Aluminum Powder Metallurgy Alloys
Fatigue Crack Propagation
Fatigue Threshold
Crack Closure

20. ABSTRACT (Continue on reverse side if necessary and identify by block number)

Experimental work on the fatigue crack growth characteristics of high strength P/M aluminum alloys has been extended, with particular attention given to crack closure in the near threshold region as a function of R. It has been conclusively shown that the R-dependence of the threshold level is directly related to closure. In the absence of closure as in ultra-fine grained material the threshold level is independent of the R-ratio. Experimental work has been initiated on the growth of fatigue cracks under variable amplitude loading conditions.

DD FORM 1 JAN 73 1473 EDITION OF 1 NOV 65 IS OBSOLETE
S/N 0102-014-6601

Unclassified

SECURITY CLASSIFICATION OF THIS PAGE (When Data Entered)

An approach to deal with topics such as the anomalous growth of short cracks, the non-propagation of cracks from notches, fatigue notch sensitivity, and the notch size-effect in fatigue has been developed. This approach is based upon the development of crack closure in the wake of a newly formed fatigue crack.

A comparison of the fatigue behavior of powder metallurgy and ingot metallurgy products has been initiated. Thus far our work indicates that P/M products can be produced which are free from manufacturing defects which might degrade fatigue properties of these high strength aluminum alloys. The fatigue properties are responsive to grain size, fracture toughness, and the degree of closure developed.

Annual Report

on

The Fatigue of Powder Metallurgy Alloys

U. S. Air Force Grant No. AFOSR 81-0046

Covering Period

1 December 1982 to 30 November 1983

Submitted to

The Air Force Office of Scientific Research

AFOSR/NE

Bolling AFB

Washington, DC 20332

Attn: Dr. Alan H. Rosenstein
Program Manager

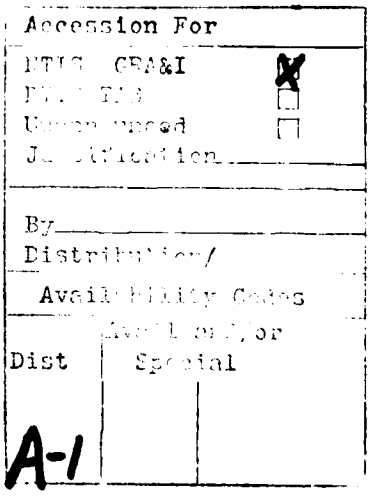

Submitted by

Professor A. J. McEvily, Jr.
Metallurgy Department U-136
University of Connecticut
Storrs, Connecticut 06268
(203) 486-2941

January 1984

ABSTRACT

Experimental work on the fatigue crack growth characteristics of high strength P/M aluminum alloys has been extended with particular attention given to crack closure in the near threshold region as a function of R. It has been conclusively shown that the R-dependence of the threshold level is directly related to closure. In the absence of closure as in ultra-fine grained material the threshold level is independent of the R-ratio. Experimental work has been initiated on the growth of fatigue cracks under variable amplitude loading conditions.

An approach to deal with topics such as the anomalous growth of short cracks, the non-propagation of cracks from notches, fatigue notch sensitivity, and the notch size-effect in fatigue has been developed. This approach is based upon the development of crack closure in the wake of a newly formed fatigue crack.

A comparison of the fatigue behavior of powder metallurgy and ingot metallurgy products has been initiated. Thus far our work indicates that P/M products can be produced which are free from manufacturing defects which might degrade fatigue properties of these high strength aluminum alloys. The fatigue properties are responsive to grain size, fracture toughness, and the degree of closure developed.

INTRODUCTION

This report covers the third year of a program of research aimed at improving our understanding of fatigue processes in powder metallurgy (P/M) alloys of interest in structural applications. During this period attention has been focused on extending the experimental data and on using the insights gained from our studies of crack closure behavior in the near-threshold region to develop an approach to treat topics such as the anomalous growth of short cracks, fatigue notch sensitivity, the fatigue notch size effect, and non-propagating fatigue cracks. We have also initiated a comparison of the fatigue properties of P/M and ingot metallurgy (I/M) high strength aluminum alloy products.

MATERIALS AND TESTS

The following alloys were obtained from the Lockheed-California Company:

P/M X7090-T6

P/M X7091-T7E69

I/M 7075-T6

These alloys were in the form of extrusions produced by Alcoa. In addition an I/M aluminum-lithium alloy, 2020-T651, was provided by Alcoa. A mechanically alloyed, IN 9021-T4 was procured from Novamet, the producer, in the form of a forged plate. The nominal chemical compositions for these materials are given in Table I. The tensile properties as determined in our laboratory are given in Table II.

P/M and I/M IMI-829 Ti alloys for low cycle fatigue tests at elevated temperature have been received.

The experimental work in this reporting period has been concentrated on fatigue crack growth studies. The specimens for these tests were of the

ASTM compact type of effective width, W, of 57.2 mm, of half-height, H, of 34.4 mm (H/W= 0.6), and of thickness, B, of 6.3 mm. We have observed that surface residual stresses can exert a marked influence on fatigue crack growth, particularly in the extrusions. To avoid these residual stresses specimens were machined only from the interior of the starting sections. In determining the rate of fatigue crack growth and the threshold level a ΔK decreasing test was employed. In this procedure loads were reduced by 10% or less and the crack was allowed to grow a distance corresponding to at least five times the monotonic plane stress plastic zone size of the previous loading for each load decrement. ΔK was determined as the stress intensity factor, ΔK, at which no crack growth was observed for at least 2×10^6 cycles. The crack opening characteristics were also determined using the modified elastic compliance method in which the elastic compliance was electronically subtracted from the total crack opening displacement (COD) signal to increase sensitivity. This method is illustrated in Fig. 1.

RESULTS AND DISCUSSION

Experimental:

Fatigue crack growth testing of IN9021 alloy has been extended to cover three R ratios as shown in Fig. 2. It is noted that the threshold level for this alloy is independent of R ratio, a unique finding. Furthermore no crack closure could be detected in these tests. For comparison purposes the crack growth behavior and closure characteristics for P/M 7090-T6 are shown in Figs. 3 and 4. The important difference between these two alloys is grain size. In 9021 it is but 0.2 microns, whereas in 7090 it is 3 microns. This difference in grain size leads to a marked difference in fracture surface roughness, particularly in the near-threshold region. Closure in this region is related to fracture surface roughness resulting from combined Mode I and Mode II growth, but it also must relate to the

size of the facets or asperities formed. In the case of 9021 these facets are extremely small and detectable closure did not occur. The fact that in the case of 9021 there is no R dependency of the threshold level clearly shows that the R dependence is related to the closure developed. Further, the fact that a material of large grain size has a higher threshold than one of small grain size even at comparable strength levels appears to hold implications for alloy development for applications at low positive R ratios. At high R ratios the beneficial effects of closure will be less pronounced, as is seen in comparing the behavior of 7090-T6 with that of IN9021 as in Fig. 5. Additional information on the variation of K_{max}, K_{min} and K_{op} for the alloys 9021 and 7090 is given in Figs. 6 and 7.

In addition we have plotted the crack growth results for 7090 in terms of the parameter ΔK_{eff} as shown in Fig. 8. At threshold the data do not correlate in terms of this parameter, the maximum discrepancy for these data being of the order of 2:1. However, there is good correlation over a limited range at a growth rate of about 10^{-6} mm/cycle. Above this rate the curves again diverge because of the activation of additional static modes of separation at high peak stress intensity levels.

Results for two I/M alloys, 7075 and 2020, are shown in Fig. 9. The 2020 alloy was included in the program because of the development of a P/M version of this alloy, and we wanted I/M information for future comparisons. However recent information indicates that the development of the P/M version are not too promising because of the difficulty of handling Li powder. The greater crack growth resistance of 2020 is due in part to its higher modulus (77.2 GPa for 2020 vs. 71.7 GPa for 7075) as well as higher crack closure.

Experimental work has also been initiated on fatigue crack growth under variable amplitude loading conditions. We are using the Mini-Twist

program which simulates wing loading conditions of transport aircraft. This type of test work appears to be an important area for future research, particularly since work at the DVFLR has shown the crack growth characteristics to be material dependent as shown in Fig. 10 for two aluminum alloys (1). An example of our own preliminary results is shown in Fig. 11.

Analytical:

In this program a considerable experimental effort has been expended on the determination of the threshold level for macroscopic crack propagation. There has been some discussion as to the significance of this quantity, and we are now in a position to state that the threshold is a most significant quantity, particularly when coupled with data on crack closure characteristics in the near-threshold region. For example, we have found that this information allows one to bridge the gap between short and long crack propagation, to understand the physical basis for fatigue notch sensitivity, and to understand the physical basis for the notch size-effect in fatigue.

The basic idea that we are using in this approach is that when a fatigue crack is first formed there is no crack closure, but as the crack propagates crack closure quickly develops, and as a consequence the stress amplitude for propagation must be increased if the crack is to continue to propagate at a rate equal to the initial rate. In work previously reported (2) it was shown that the important closure events affecting the threshold level occurred in a distance of less than one millimeter, and for purposes of analysis we have taken this distance to be 0.5 mm, with closure occurring as in Fig. 12. It is seen that the closure varies from zero to a maximum value which corresponds to the macroscopic closure level. In this case the macroscopic level corresponds to that of a steel of medium strength,

chosen in order to compare with available data on short crack growth behavior from notches in such a material.

Many of the studies of short crack behavior involve the growth of short cracks from notches. Fig. 13 shows how the stress intensity factor varies with crack length depending on the method employed to calculate the stress intensity factor. Curve A is the exact solution for a crack growing from a circular hole (3). Curve B is the solution for a crack taken to be equal to its length, l, plus that of the radius, c. Curve C corresponds to B but with the inclusion of closure development which results in a minimum in this curve. We will make use of curve C in subsequent analysis. This involves an increase in the initial value of the stress intensity factor which is justified on the grounds that the initial crack has a relatively large plastic zone size to crack length ratio which leads to non-linear behavior and consequently a higher growth rate. We assume that an increase of the initial stress intensity level from that of curve A to that of curve B takes this into account, although this is not a cricial assumption.

Fig. 14 is a plot of log ($\Delta\sigma/2$) vs. log (c+l). The right hand portion of curve A represents the condition for the propagation of a macroscopic crack at a rate of 10^{-8} mm/cycle, i.e., the threshold level. This curve includes the effect of closure. In the absence of closure curve B results. This curve is equivalent to ΔKeffective. At the left hand end of the plot the curves bend and merge with the stress which corresponds with the endurance limit of the material. On this plot the experimental data of El Haddad et al. (4) for three hole sizes are plotted. The curves C, D, and E, are plots of the calculated stress required to propagate a crack under the influence of closure development up to its maximum value. For the two smaller holes the stress to propagate is greater than the stress to initiate, and as a result nonpropagating cracks can develop in accord with the

experimental observations. On the other hand, in the case of the largest hole the stress to initiate exceeds the stress requirement for propagation so that a non-propagating crack cannot develop in the case.

The reason for the fatigue notch size effect is also evident from this plot. Note that the stress for fatigue failure decreases monotonically from the maximum of curve C to $\Delta\sigma_{end}/2K_t$ as the hole size increases. This is the notch size effect which is important in predicting the fatigue strength of notched parts from smooth specimen data. A comparison with empirical formulations is given in Fig. 15. The basis for fatigue notch sensitivity can also be related to Fig. 14 and crack closure, for as the extent of crack closure decreases as in going from a low to a high strength steel, curve A will approach curve B. The closer these curves are, the greater the notch sensitivity. These considerations also have important implications for material selection in the presence of potential flaws. As indicated in Fig. 16 if an inspection method can screen from use components having a certain flaw size or larger then components containing flaws just below this limit may be placed in service. In such a case a material of lower strength may prove to be superior to one of higher strength under these conditions. However at high R ratios where closure may be absent the ratio will control and in this case the high strength material may be superior.

A Review of the Fatigue Properties of High-Strength P/M Aluminum Alloys

In this section a brief review of the fatigue properties, i.e., smooth and notched specimen S/N behavior and crack growth characteristics, will be given. The purpose is to determine if there are any unique features associated with powder metallurgy products per se as well as to compare the relative fatigue resistance of P/M and I/M products.

As has been pointed out (8) the rapid solidification of powders from the melt can lead to a high degree of microstructural refinement, extended solubilities of alloying elements, and the elimination of complex constituent phases. The important variables affecting the cooling rate are particle size and particle velocity. Particle sizes produced by Alcoa (9) are typically in the range of 10 to 20 microns. After processing grain sizes can range from 5 microns to 100 microns dependent upon the processing procedure in the case of the alloy 7091 (10). This alloy contains in wt.% 6.5 Zn, 2.5 Mg, 1.5 Cu, and 0.4 Co. In this alloy the dispersoid particles are Co_2Al_9 and Al_2O_3. Because of the rapid solidification of the powders, the dispersoids as well as the secondary constituent particles are less than 0.5 microns in size. In contrast the size of secondary constituent paticles containing Fe and Si can be in the range of 10 microns in I/M products. Improved fatigue resistance can be anticipated as the size of these particles is reduced. The minimization of segregation in rapidly solidified powders is also important in aluminum Al-Li alloys. These alloys are of interest because of a higher Young's modulus (77.2 GPa for 2020 vs. 71.7 GPa for 7075) at a lower density (2.71×10^3 Kg/m^3 for 2020 vs. 52.80×10^3 Kg/m^3 for 7075). In the ingot metallurgy product segregation of Lithium causes reduction in fracture toughness and ductility. There is some evidence that the P/M product can develop improved toughness and density (11). (K_Q for I/M was 22 MPa$\sqrt{m}$ vs 31MPa$\sqrt{m}$ for P/M. The percent elongation for I/M was 3 pct. vs. 5 pct. for P/M).

Fig. 17 presents a comparison of the fatigue behavior of P/M Al-6.5 Zn-2.3Mg-2.0Cu alloy and I/M 7075 (12), and the fatigue properties of the P/M material are seen to compare most favorably with those of the I/M material. In the case of a 2024 + 3% Li RS alloy the fatigue strength to tensile strength ratio was reported to be in excess of 0.5, whereas the

usual ratio is in the range of 0.3 to 0.35 for aluminum ingot alloys (8). Our own studies have also shown that the P/M 7090 T6 and 7091 T7E69 alloys can be superior to a I/M 7075 T76 alloy by approximately 20% at least in smooth specimen performance at R=-1, at a fatigue lifetime of 10^7 cycles. The fatigue notch sensitivity must also be considered. As shown in Fig. 18 the fatigue life of the P/M aluminum alloy X7091-T7E69 is greater than the conventional I/M aluminum alloy 7075-T76510 (13). However, if the P/M alloy were to be produced such that the grain size was in the sub-micron range, i.e. IN9021, the comparison might be less favorable due to absence of crack closure.

The refined microstructure of rapidly solidified aluminum powders as well as the oxide coatings on these powders can influence the fatigue crack initiation process. For example, in a conventionally processed I/M alloy, 2024-T4, Kung and Fine (14) have observed that the probability of initiating a fatigue crack at constituent particles dropped down rapidly as the inclusion size decreased below 6 microns. This probability was quite small for 2 micron sized inclusions, the smallest size measured. Below this size it was difficult to distinguish constituent particles from dispersoids added for grain refinement. The initiation mode was along slip bands which emanated from the inclusions. In coarse grained 2124 heat treated to minimize the constituent particle size, slip band fatigue cracks unassisted by inclusions formed more easily than in the finer grained 2024. From such findings both a fine grain size as well as the absence of large intermetallic inclusions are needed for high resistance to fatigue crack initiation. These characteristics are present in rapidly solidified powders, but the presence of an oxide coating on the powders may have an adverse effect. For example in P/M X7091 fatigue cracks initiated at grain boundaries due to the segregation of Al_2O_3 particles formed during atomization and subse-

quently segregated to some grain boundaries. In other cases the oxides as viewed by TEM are thoroughly broken up and dispersed by the working process and would therefore be expected to have less influence on fatigue crack initiation. In our work with these alloys in fatigue crack propagation the path in the near-threshold region is transgranular with the possible exception of X7091 which developed pronounced fretting debris and indications of intergranular fracture.

In contrast to the X7091 P/M alloy studied by Hirose and Fine (10), Griffith and Santer (15) studied the behavior of the same alloy but with a much greater extent of foreign contamination which came from either the powder production process or subsequent handling before the material was densified. Air atomized powders were involved in the Griffith and Santer study; the powder production procedure used in preparing the material studied by Fine was not specified. Griffith and Santer conducted axial fatigue tests at R=0.1 in the life range of 10^3 to 10^6 cycles. Specimens with abnormally short fatigue lives had surface defects greater than 50 microns in diameter of several smaller, closely spaced inclusions acting in tandem. Long-lived specimens had surface inclusions less than 30 microns in diameter. Three types of initiating defects were identified: aluminum rich oxides (60% occurrence), transition metal inclusions (30% occurrence), and microstructural boundaries. Improved quality control during manufacture should serve to minimize the occurrence of these defects.

A comparison of fatigue crack growth characteristics of P/M and I/M alloys is given in Fig. 19. In comparison to the I/M 7075 alloy the P/M alloys may be slightly better or worse dependent upon the range of crack growth. In the near threshold region the P/M alloys X7090 and X7091 exhibit greater resistance to fatigue crack growth than the I/M alloy. However the ultra-fine grained IN9021 which does not develop crack closure

is not as good. In the intermediate range the I/M alloy is slightly superior to all three of the P/M alloys. In this range this superiority results from two causes; a higher degree of crack closure, i.e., a lower value of ΔK_{eff} as well as a higher fracture toughness.

References

1. K. Schulte, K.-H. Trautmann, H. Nowack, Presented at the Intl. Conf. on Anaytical and Experimental Fracture Mechanics, Rome, June, 1980.
2. K. Minakawa, J. C. Newman, Jr. and A. J. McEvily, Fatigue of Engng. Mater. and Struct., Vol. 6, No. 4, p. 359, 1983.
3. H. Tada, P. C. Paris and G. R. Irwin, The Stress Analysis of Cracks Handbook, Del Research Corp., Hellertown, PA, 1973.
4. M. H. El Haddad, T. H. Topper and K. N. Smith, Engng. Frac. Mech., 11, p. 573, 1979.
5. H. Neuber, Kerbspannungslehre, Springer, 1958.
6. P. Kuhn and H. F. Hardrath, NASA Tech. Note 2805, 1952.
7. R. E. Peterson, Stress Concentration Factors, John Wiley and Sons, New York, 1974.
8. N. J. Grant, in "High Strength Powder Metallurgy Aluminum Alloys", Conf. Proc., M. T. Koczak and G. J. Hildeman, Eds., AIME, p. 3, 1982.
9. W. L. Otto, Jr. "Metallurgical Factors Controlling Structure in High Strength P/M Products", Technical Reprot AFML-TR-76-60 May, 1976.
10. S. Hirose and M. E. Fine, in "High Strength Powder Metallurgy Alloys" Conf. Proc., M. J. Koczak and G. J. Hildeman, Eds., AIME, p. 19, 1982.
11. P. S. Pao, K. K. Sankaran and J. E. O'Neal, in "Aluminum-Lithium Alloys" Conf. Proc. T. H. Sanders, Jr. and E. A. Starke, Jr., Eds., AIME, p. 307, 1981.
12. J. P. Lyle, Jr. and W. S. Cebulak, Metals. Engng. Quarterly, February, p. 52, 1974.
13. S. L. Langenbeck, in "High Strength Powder Metallurgy Aluminum Alloys" Conf. Proc., M. J. Koczak and G. J. Hildeman, Eds., AIME, p. 87, 1982.

14. C. Y. Kung and M. E. Fine, Met. Trans, A, 10A, p. 603, 1979.

15. W. M. Griffith and J. S. Santner, in "High Strength Powder Metallurgy Aluminum Alloys" Conf. Proc., M. J. Koczak and G. J. Hildeman, Eds., AIME, p. 125, 1982.

Papers Published

1) A. J. McEvily, "On the Quantitative Analysis of Fatigue Crack Propagation", ASTM STP811 p. 283, 1983.
2) K. Minakawa, J. C. Newman, Jr. and A. J. McEvily, "A Critical Study of the Crack Closure Effect on Near-Threshold Fatigue Crack Growth", Fatigue of Engng. Mater. and Struct. Vol. 6, No. 4, p. 359, 1983.
3) A. J. McEvily and K. Minakawa, "Crack Closure and the Growth of Short and Long Fatigue Cracks", Scripta Metall. Vol. 18, p. 71, 1984.

Papers Submitted

1) A. J. McEvily and K. Minakawa, "On the Role of Crack Closure in Fatigue Crack Growth", to be published in Proc. of ICF Symposium on Fracture Mechanics. Beijin, November, 1983.
2) A. J. McEvily and K. Minakawa, "Crack Closure and the Conditions for Fatigue Crack Propagation", to be published in "Fatigue Crack Growth Threshold Concepts", Proc. of Intl. Symposium, AIME, Philadelphia, October, 1983.
3) A. J. McEvily, "Fracture Prevention in the Motor Vehicle Industries", to be published in Proc. of Intl. Conf. on Fracture Prevention in Energy and Transport Systems, December, 1983.

Papers in Preparation

1) K. Minakawa, G. Levan and A. J. McEvily, "The Influence of Load Ratio on Fatigue Crack Growth Rates in 7090-T6 and IN9021-T4 Aluminum Alloys.

Presentations

1) K. Minakawa and A. J. McEvily, "Near-Threshold Fatigue Crack Growth in Aluminum Alloys in Air and 3.5 pct. NaCl solution, TMS-SIME 112th Annual Meeting, Atlanta, March, 1983.
2) A. J. McEvily and K. Minakawa, "Crack Closure and the Conditions for Fatigue Crack Propagation, Intl. Sympo. on Fatigue Crack Growth Threshold Concepts, Philadelphia, October, 1983.
3) A. J. McEvily, "Fracture Prevention in the Motor Vehicles Industries", Intl. Conf. on Fracture Prevention in energy and Transport Systems, Rio de Janeiro, November, 1983.

Personnel

Principal Investigator:	A. J. McEvily, Professor
Associate Investigator:	K. Minakawa, Asst. Professor in Residence
Research Technician:	R. Shover
M.S. Candidate:	G. Levan

Figure Captions

Fig. 1 Schematic diagram of the modified compliance method.

Fig. 2 Fatigue crack growth rate, da/dN, as a function of ΔK for the IN9021-T4 aluminum alloy at three R ratios.

Fig. 3 Fatigue crack growth rate, da/dN, as a function of ΔK for the 7090-T6 aluminum alloy at three R ratios.

Fig. 4 Crack opening level in terms of the ratio of K_{op} to K_{max} as a function of ΔK for the 7090-T6 aluminum alloy at three R ratios.

Fig. 5 Comparison of fatigue threshold levels for the IN9021 and 7090 alloys at three R ratios.

Fig. 6 K_{max}, K_{min} and K_{op} as a function of R for the IN9021-T4 alloy. In this alloy K_{op} is equal to K_{min}.

Fig. 7 K_{max}, K_{min} and K_{op} as a function of R for the 7090-T6 alloy.

Fig. 8 Fatigue crack growth rate, da/dN, as a function of ΔK_{eff} for the 7090-T6 alloy.

Fig. 9 Fatigue crack growth rate, da/dN, as a function of ΔK for two I/M alloys, 7075-T76 and 2020-T651.

Fig. 10 Crack length as a function of number of flights under the Mini-Twist loading program for two Al-Zn-Mg alloys.

Fig. 11 Crack length as a function of number of flight under the Mini-Twist loading program.

Fig. 12 Assumed development of closure as a short crack extends from zero length to a length of 0.5 mm.

Fig. 13 Variation of $\Delta K/\Delta\sigma$ as a function of crack length, l, for threee cases.

Fig. 14 Crack propagation conditions as a function of total crack length c+l and stress amplitude.

Fig. 15 Variation of K_F as a function of hole radius for three cases; (A) based on the present analysis; (B) based on $K_F = 1 + \frac{K_T - 1}{1 + \sqrt{\rho'/\rho}}$ (5)(6), (ρ' = 0.4 mm); (c) based on $K_F = 1 + \frac{K_T - 1}{1 + \frac{\alpha_o}{\rho}}$ (7) (α_o = 0.25 mm).

Fig. 16 Effect of strength level and crack closure on the allowable stress from non-propagation of a crack as influenced by inspection capability.

Fig. 17 A comparison of the fatigue behavior of P/M Al-6.5Zn-2.3Mg-2.0Cu and I/M 7075 T6 alloys.

Fig. 18 A comparison of the fatigue notch sensitivity of the P/M X7091-T7E69 and the I/M 7075-T76510 alloys.

Fig. 19 A comparison of fatigue crack growth characteristics of P/M and I/M alloys.

Table I Nominal Chemical Compositions (Wt%)

	Cu	Mg	Mn	Si	Fe	Co	Zn	Ti	Cr	C	O	Cd	Li
X7090 T6	0.60-1.30	2.00-3.00		max 0.12	max 0.15	1.00-1.90	7.30-8.70						
X7091 T7E69	1.20-2.00	2.20-3.00		max 0.15	max 0.20	0.20-0.60	6.00-7.00						
7075 T76	1.20-2.00	2.10-2.90	max 0.30	max 0.40	max 0.50		5.10-6.10	max 0.20	0.18-0.28				
1N9021 T4	4.00	1.50		0.05	0.20					1.10	0.80		
2020 T651	4.50		0.50									0.20	1.10

Table II Tensile Properties

	Orientation	σ_{ys}(MPa)	UTS(MPa)	Elongation (%)[1]
X7090 T6	L[2]	650	683	8.5
	LT[3]	580	634	8.2
X7091 T7E69	L	544	593	13
	LT	527	580	12
7075 T76	L	471	540	7
	LT	420	461	6
1N9021 T4	L	535	600	7.2
	LT	523	587	8.3
2020 T651[4]	L	516	545	4.8
	LT	515	525	0.9

(1) 25.4 mm
(2) L: Longitudinal
(3) LT: Long-transverse
(4) Determined by Alcoa.

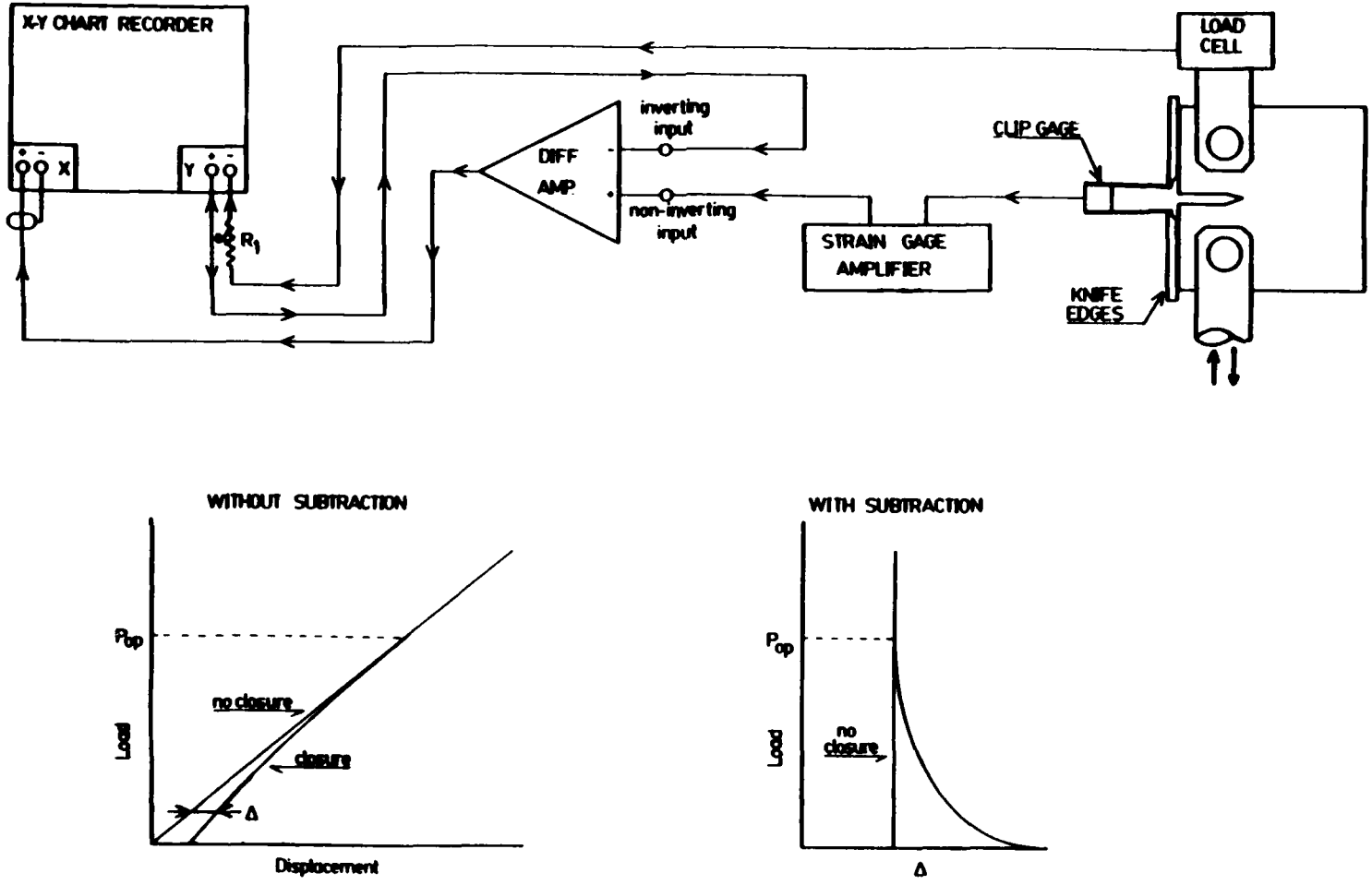

Fig. 1 Schematic diagram of the modified compliance method.

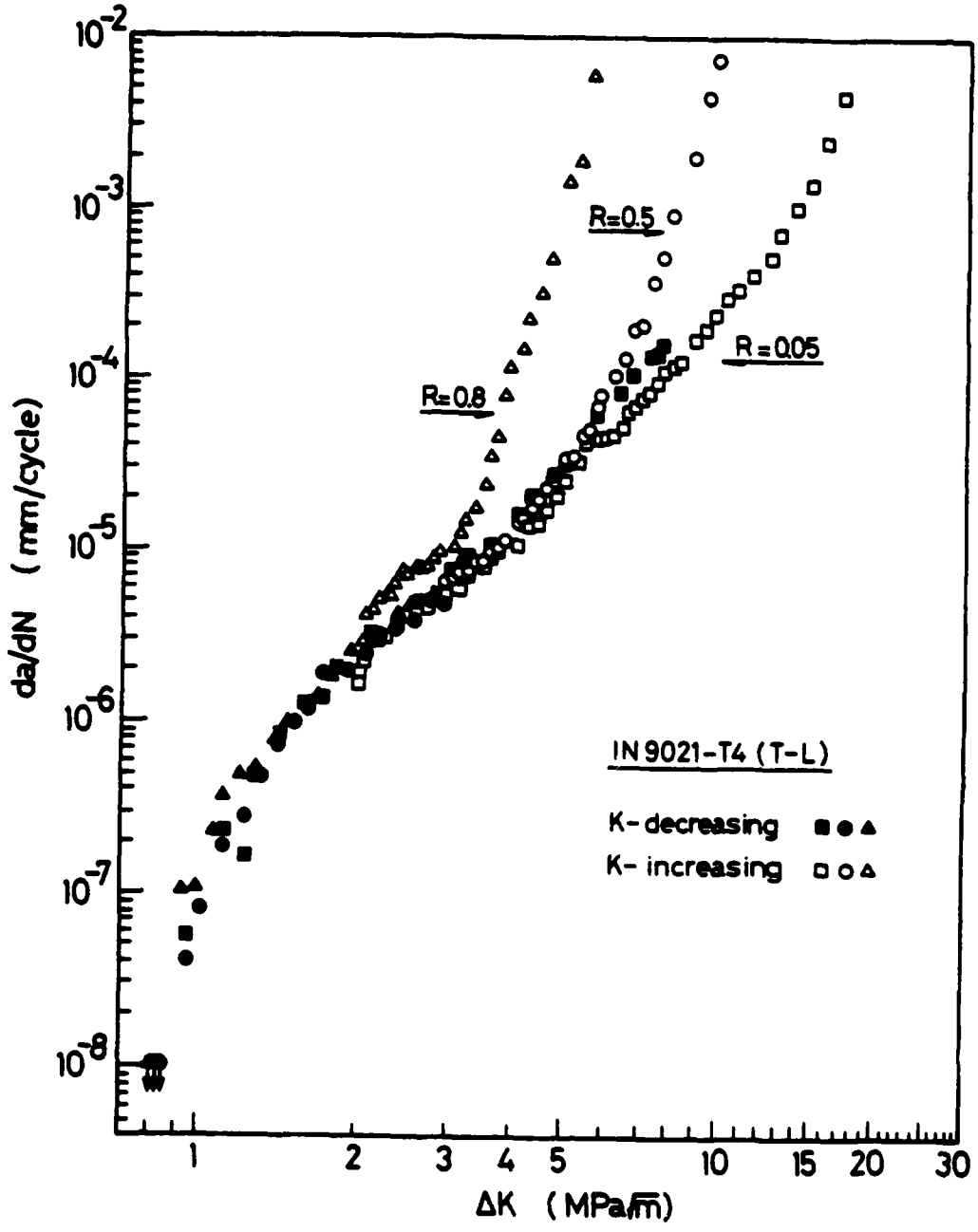

Fig. 2 Fatigue crack growth rate, da/dN, as a function of ΔK for the IN9021-T4 aluminum alloy at three R ratios.

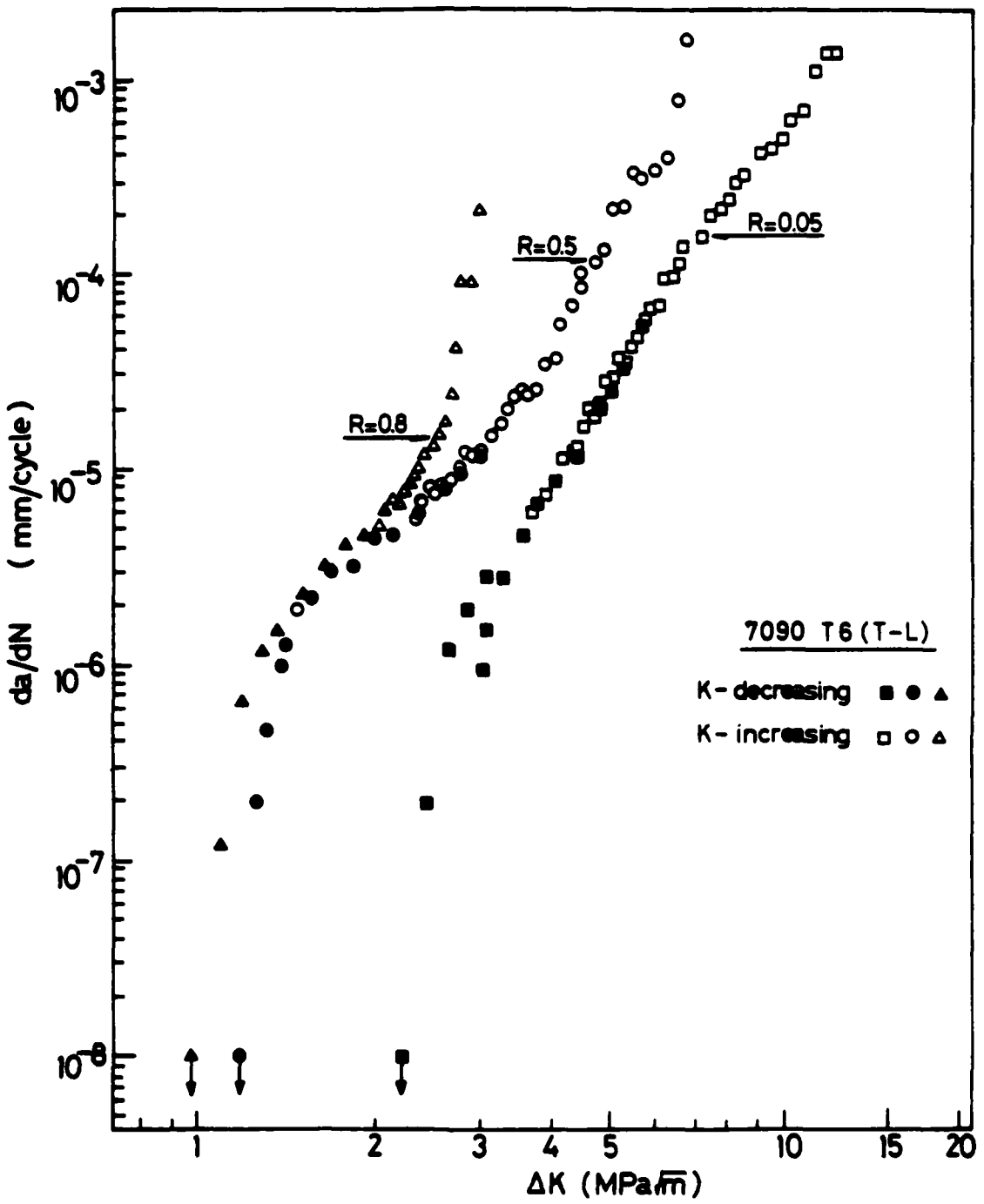

Fig. 3 Fatigue crack growth rate, da/dN, as a function of ΔK for the 7090-T6 aluminum alloy at three R ratios.

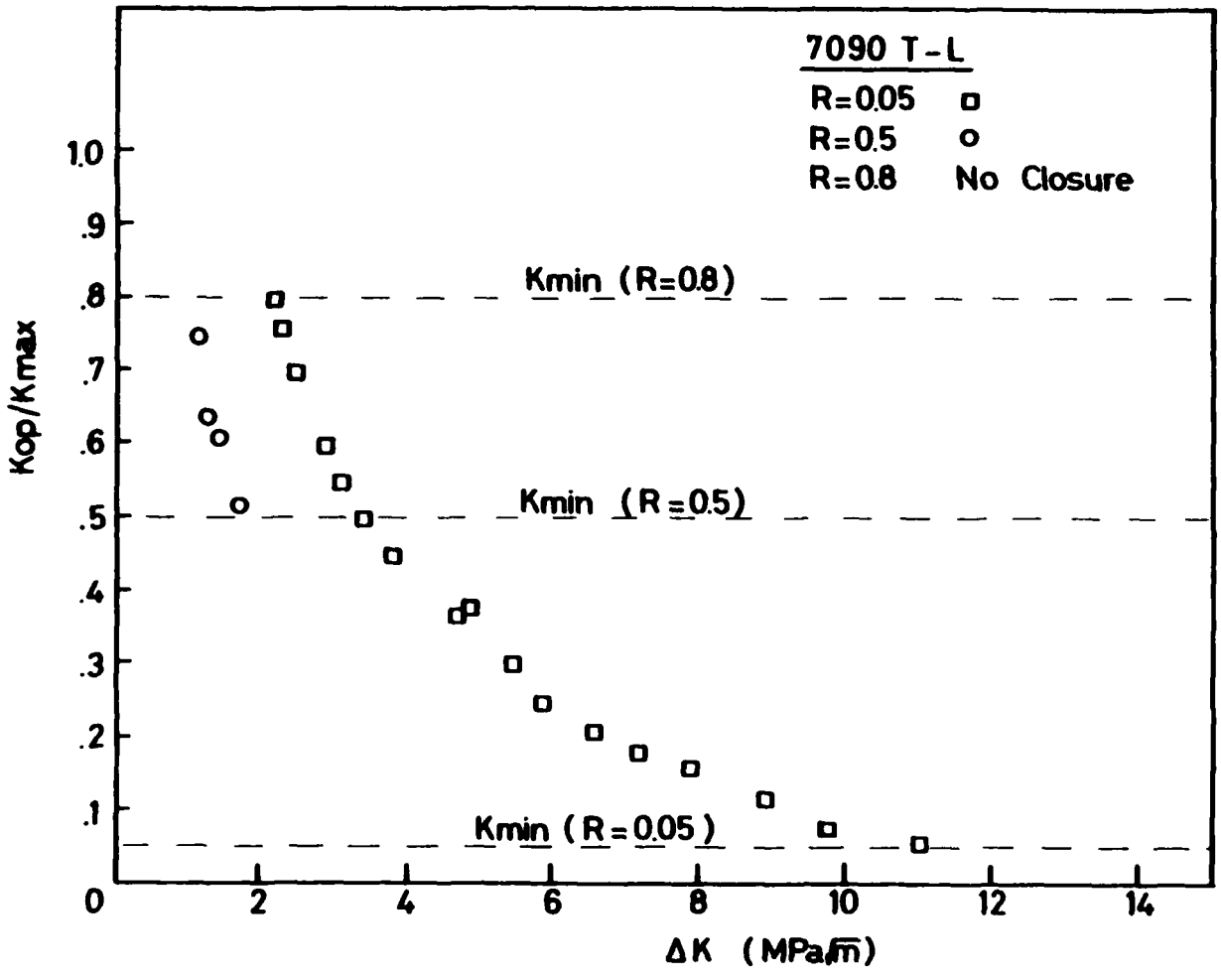

Fig. 4 Crack opening level in terms of the ratio of K_{op} to K_{max} as a function of ΔK for the 7090-T6 aluminum alloy at three R ratios.

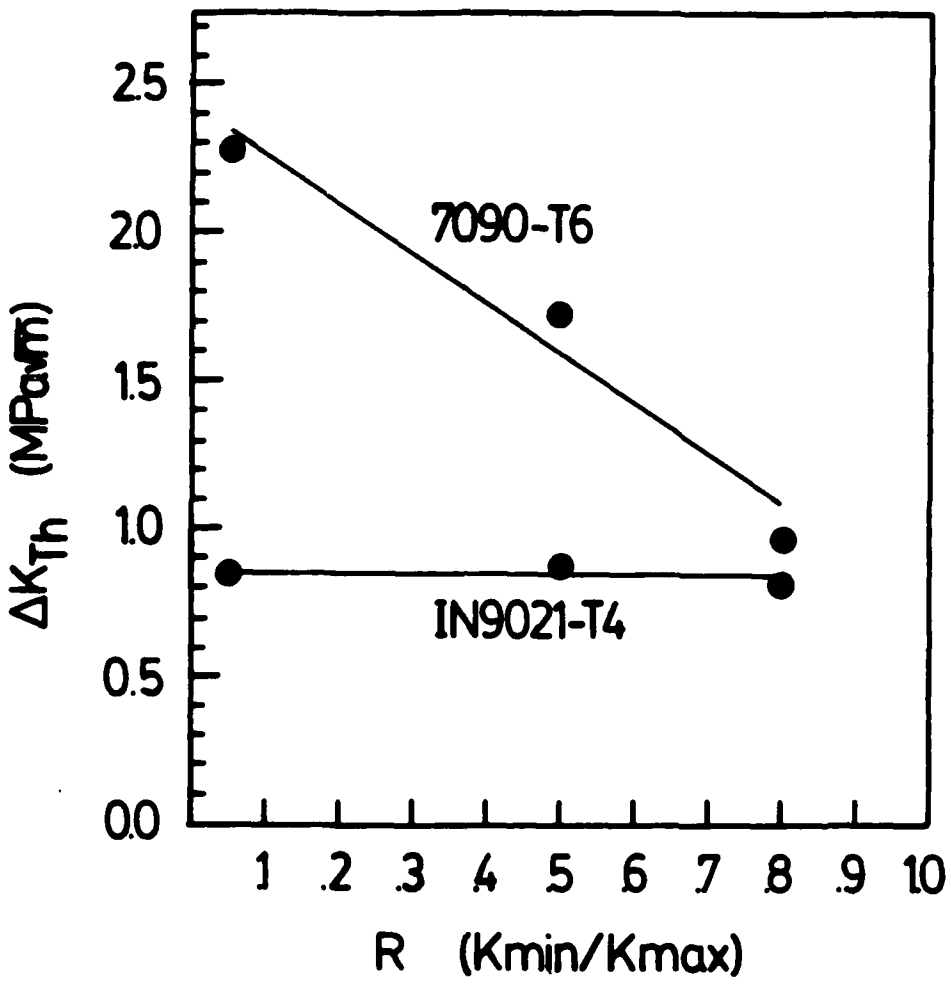

Fig. 5 Comparison of fatigue threshold levels for the IN9021 and 7090 alloys at three R ratios.

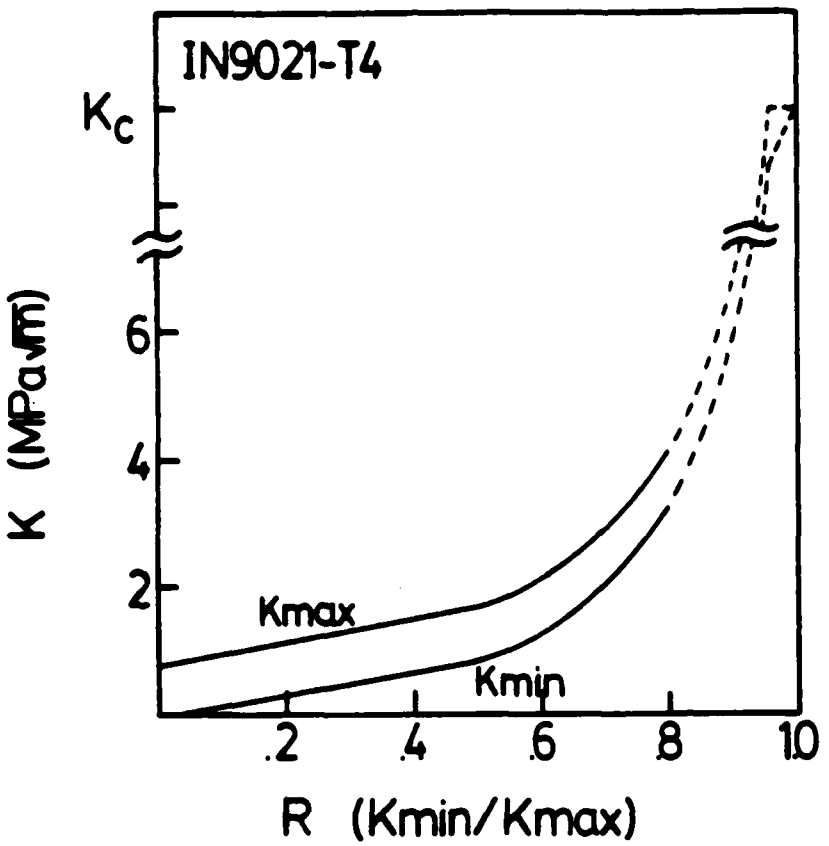

Fig. 6 K_{max}, K_{min} and K_{op} as a function of R for the IN9021-T4 alloy. In this alloy K_{op} is equal to K_{min}.

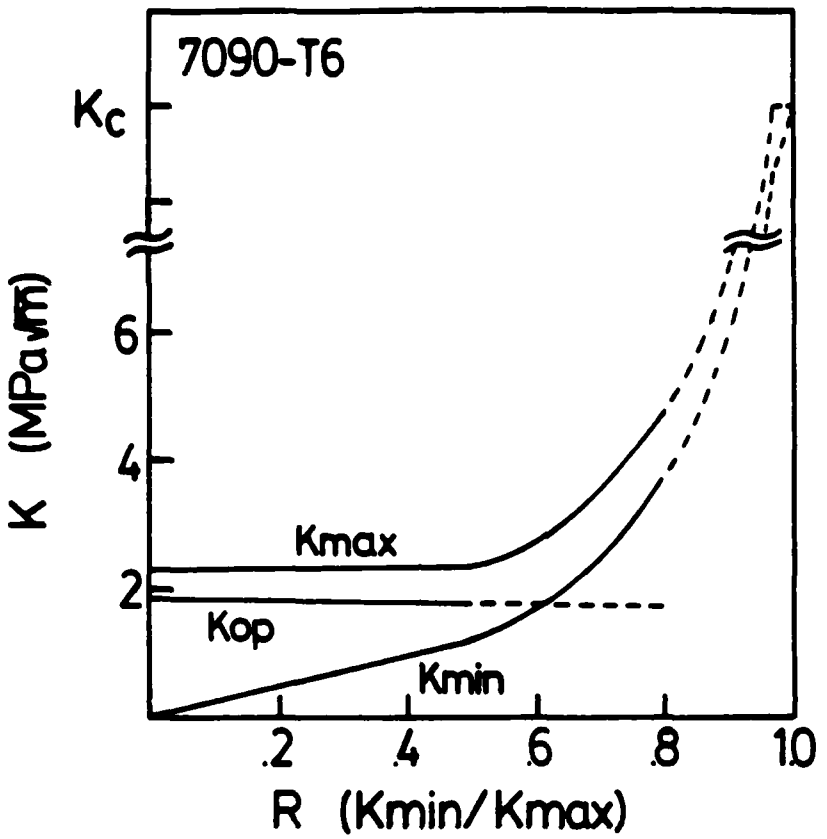

Fig. 7 K_{max}, K_{min} and K_{op} as a function of R for the 7090-T6 alloy.

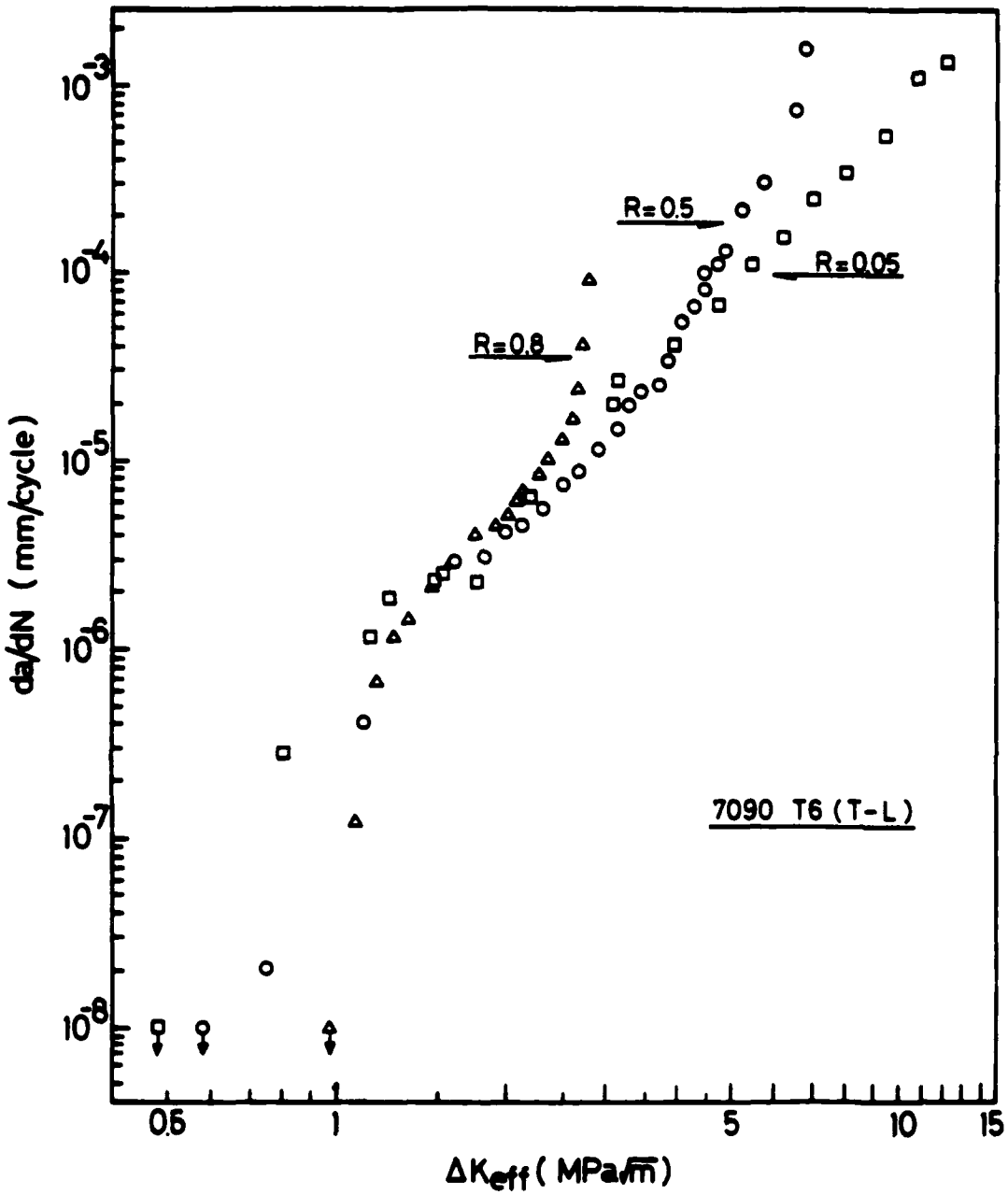

Fig. 8 Fatigue crack growth rate, da/dN, as a function of ΔK_{eff} for the 7090-T6 alloy.

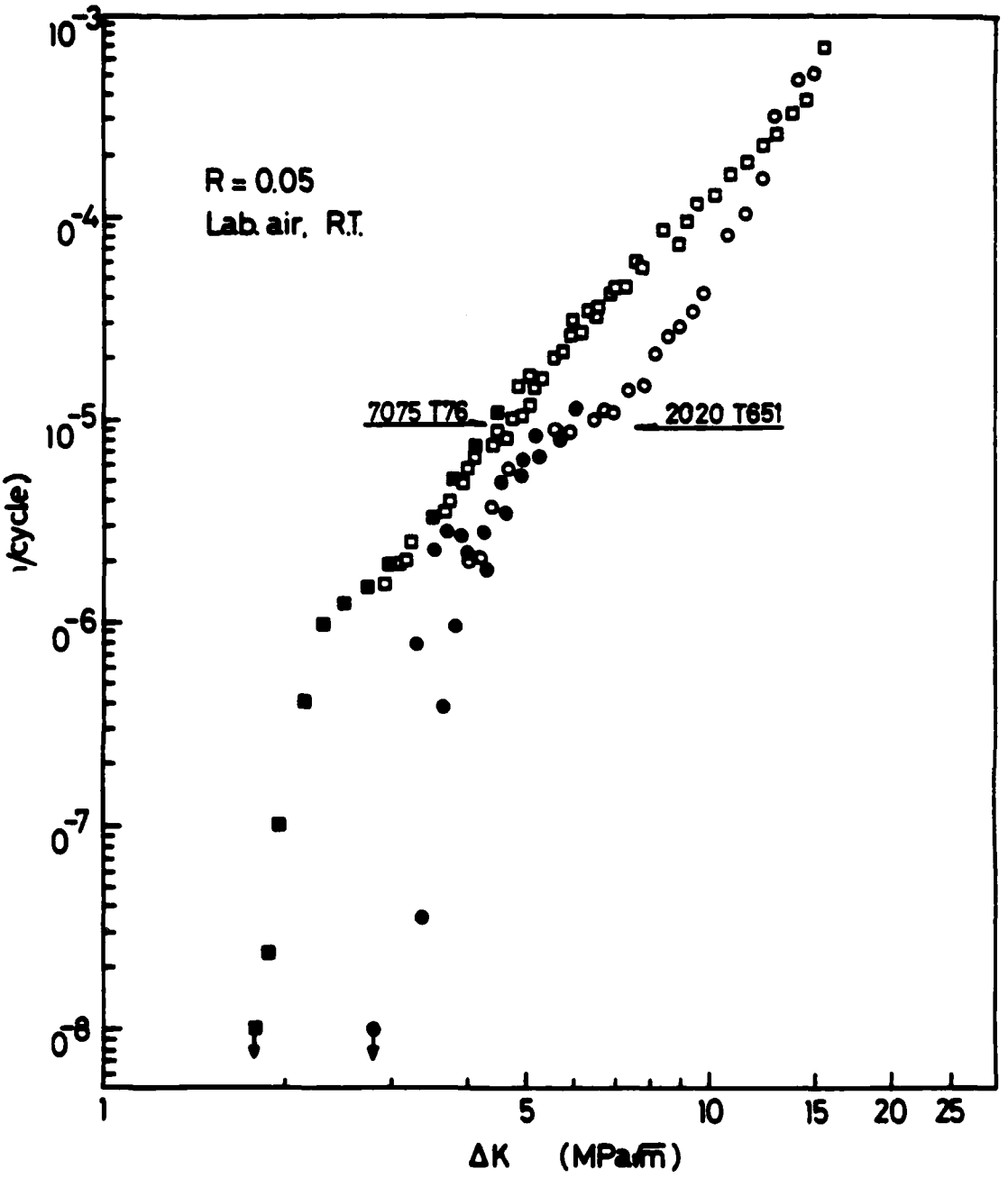

Fig. 9 Fatigue crack growth rate, da/dN, as a function of ΔK for two I/M alloys, 7075-T76 and 2020-T651.

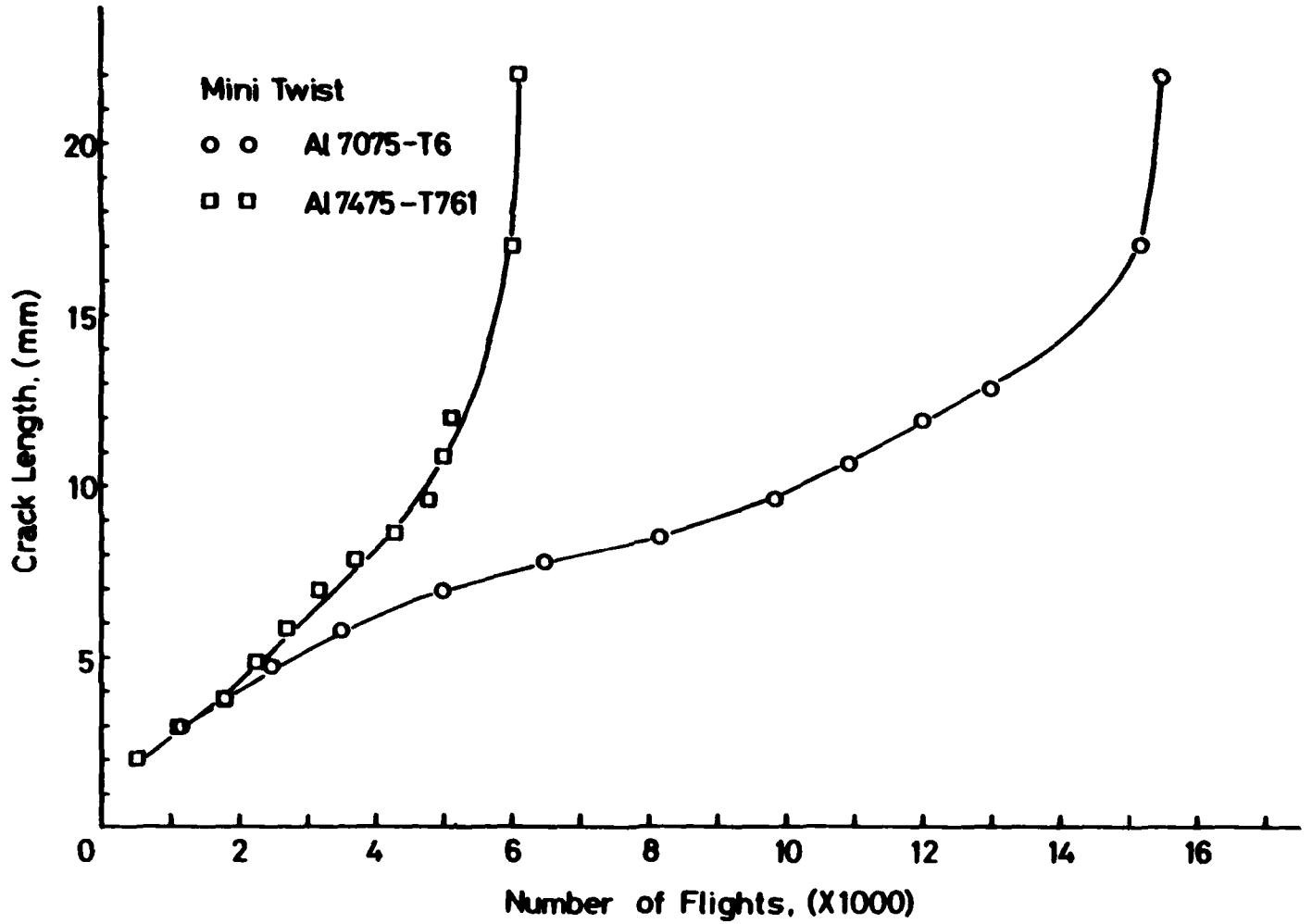

Fig. 10 Crack length as a function of number of flights under the Mini-Twist loading program for two Al-Zn-Mg alloys.

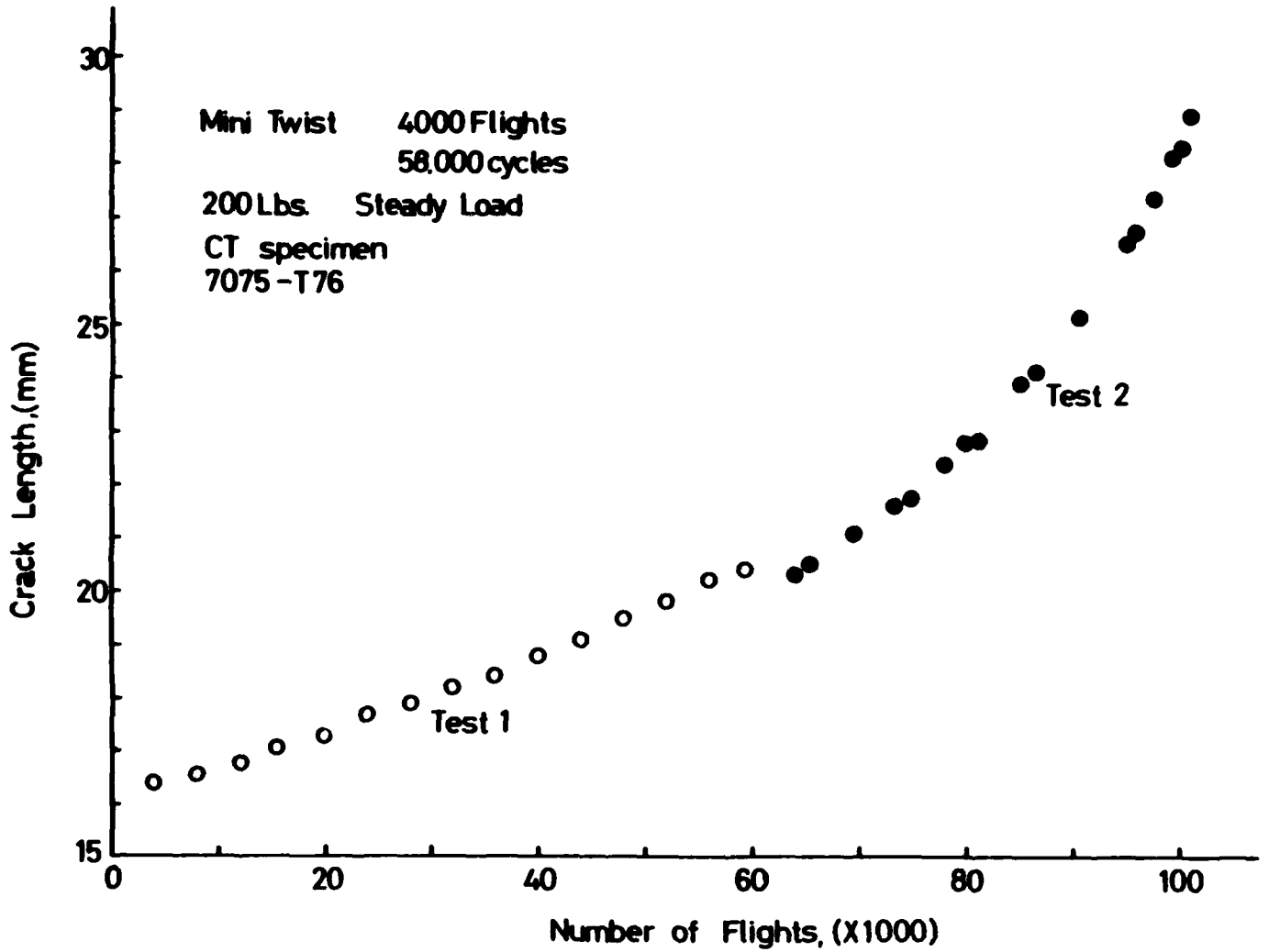

Fig. 11 Crack length as a function of number of flight under the Mini-Twist loading program.

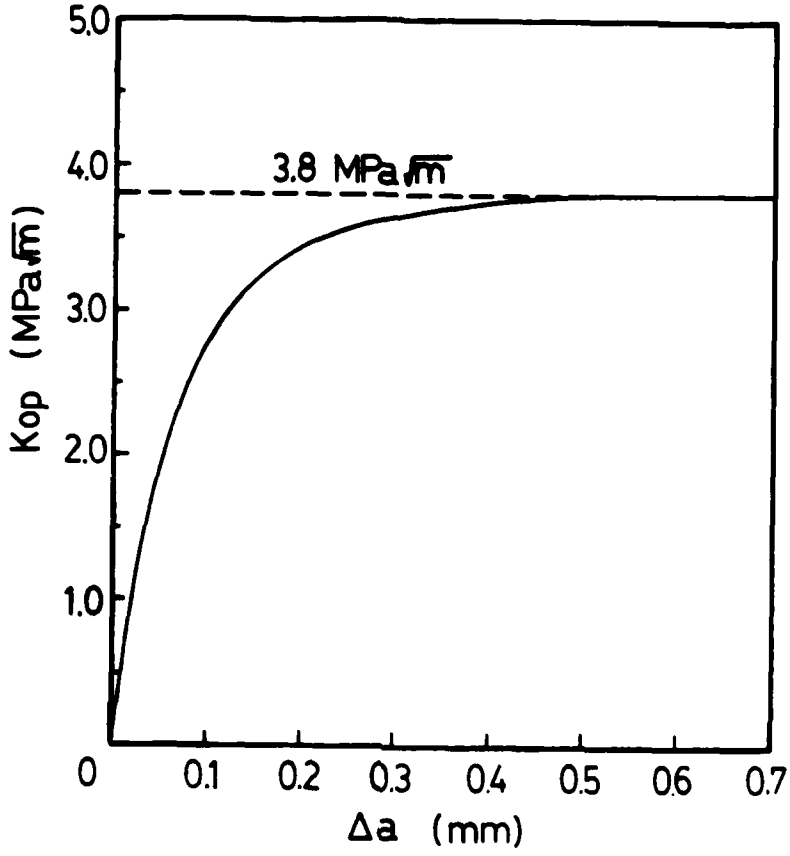

Fig. 12 Assumed development of closure as a short crack extends from zero length to a length of 0.5 mm.

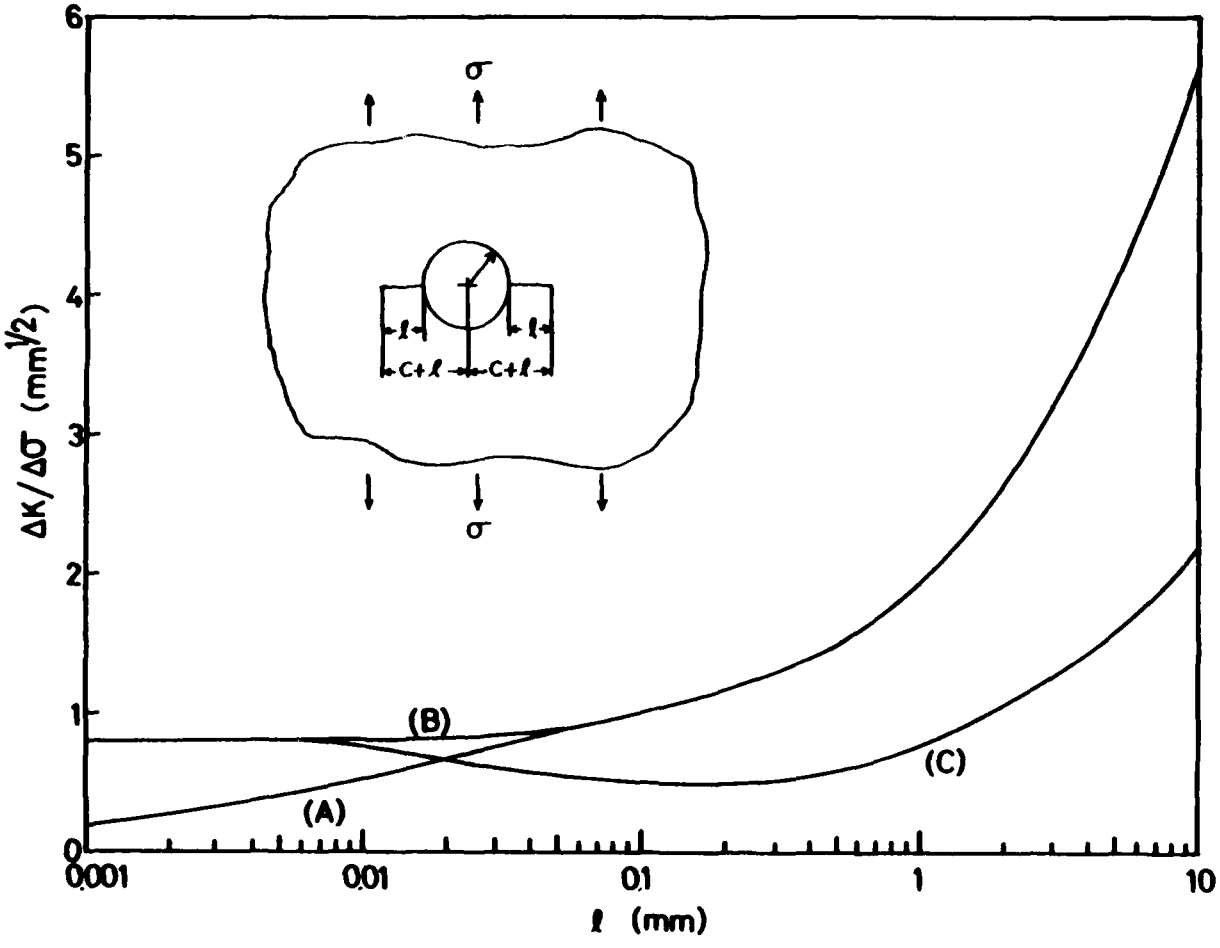

Fig. 13 Variation of $\Delta K/\Delta\sigma$ as a function of crack length, l, for threee cases.

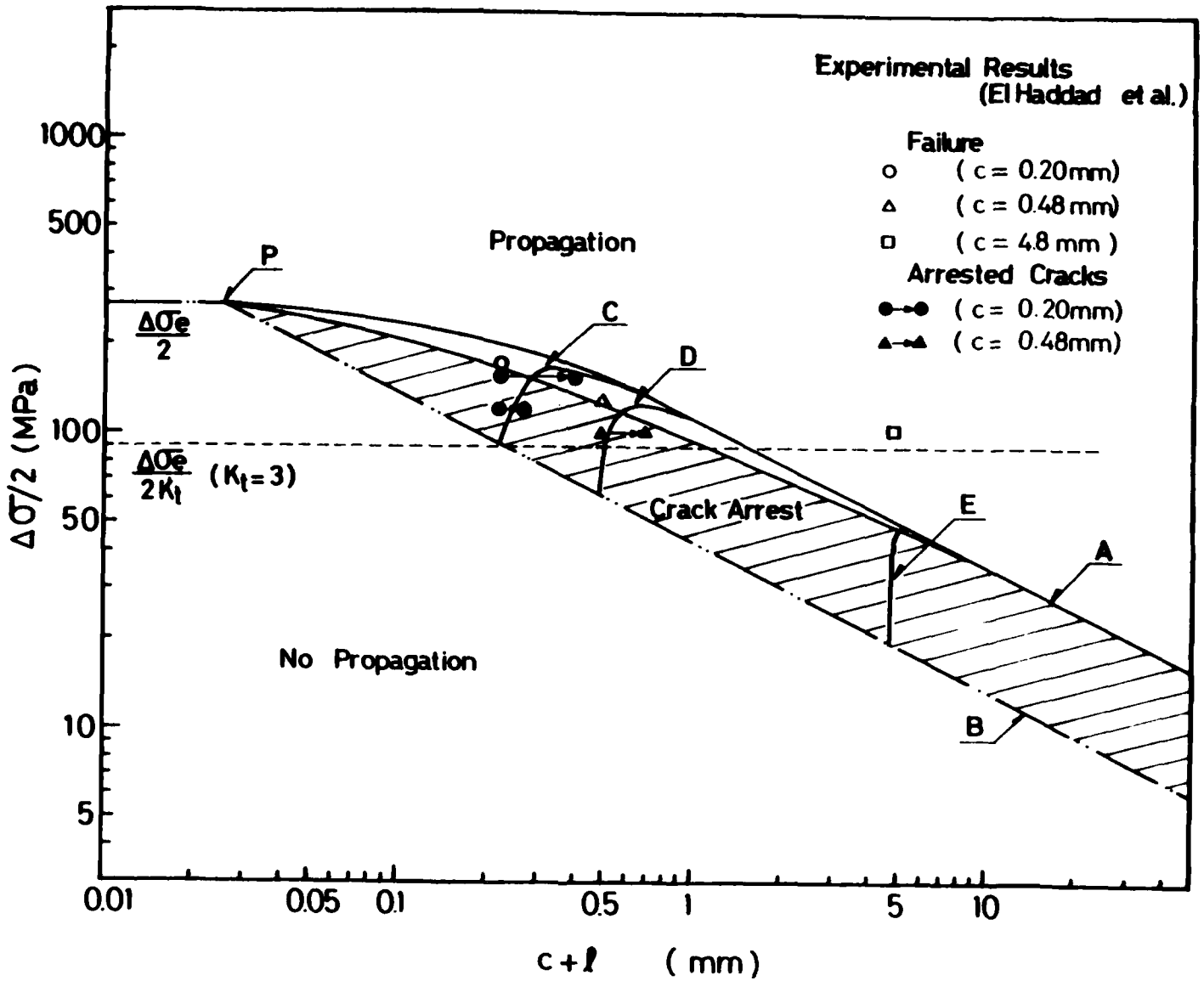

Fig. 14 Crack propagation conditions as a function of total crack length c+l and stress amplitude.

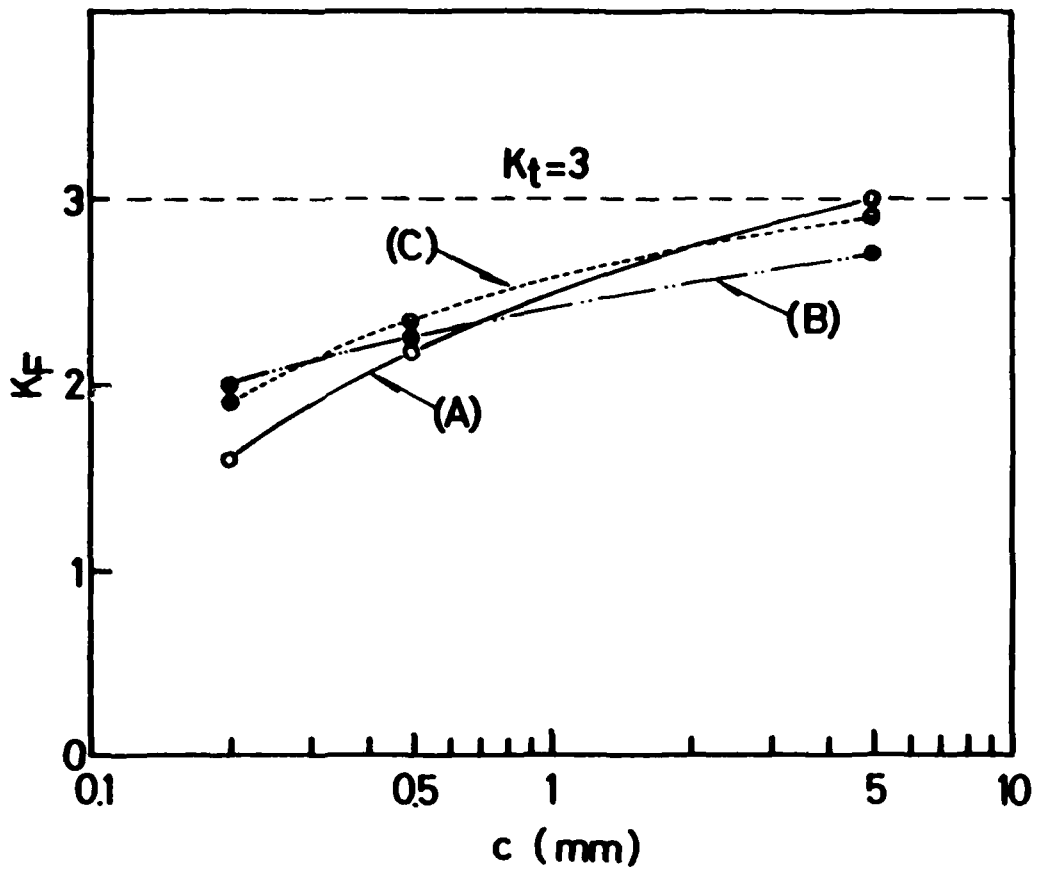

Fig. 15 Variation of K_F as a function of hole radius for three cases; (A) based on the present analysis; (B) based on

$$K_F = 1 + \frac{K_T - 1}{1 + \sqrt{\rho'/\rho}}$$ (5)(6) (ρ' = 0.4 mm); (c) based on $K_F = 1 + \frac{K_T - 1}{1 + \frac{\alpha_o}{\rho}}$ (7)

(α_o = 0.25 mm).

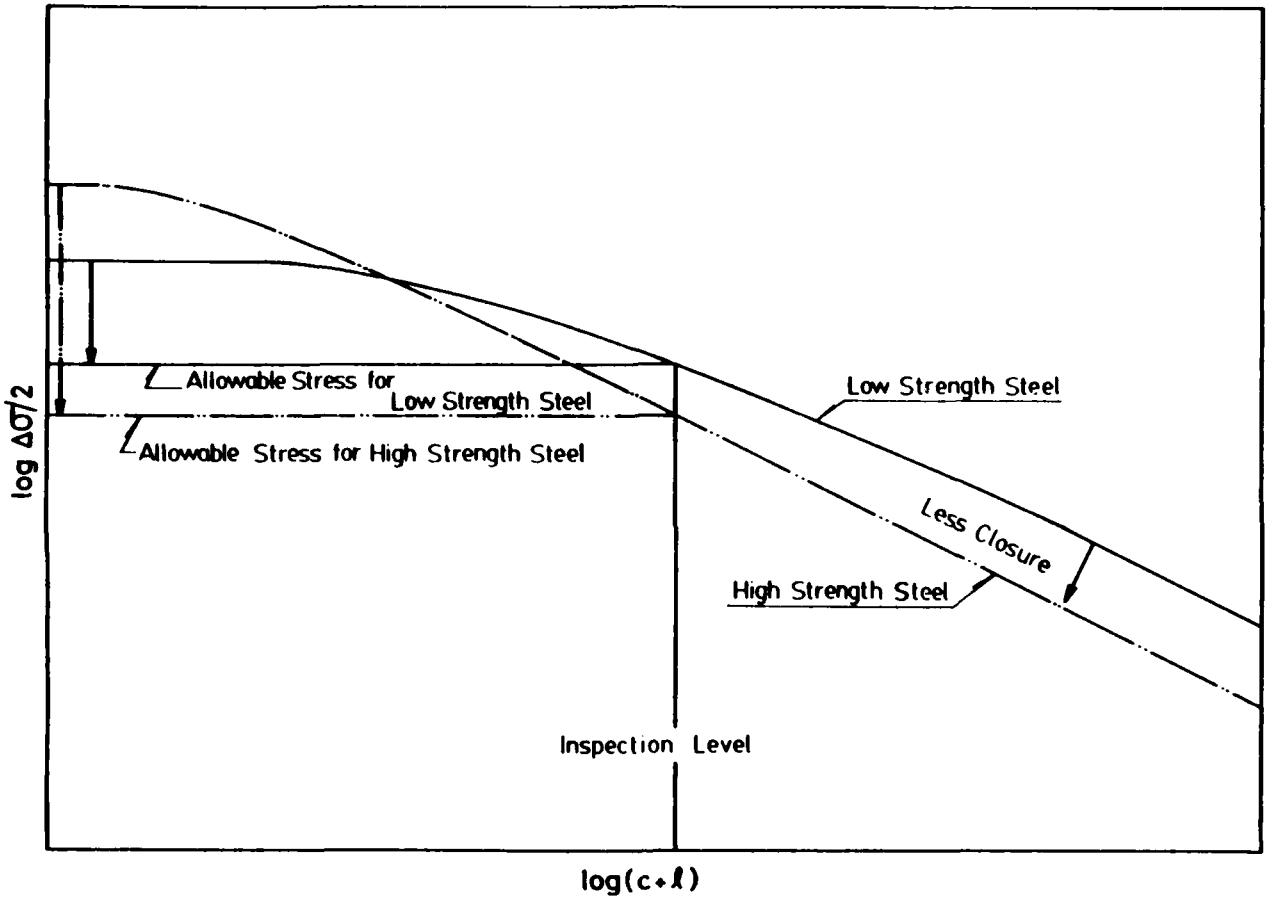

Fig. 16 Effect of strength level and crack closure on the allowable stress from non-propagation of a crack as influenced by inspection capability.

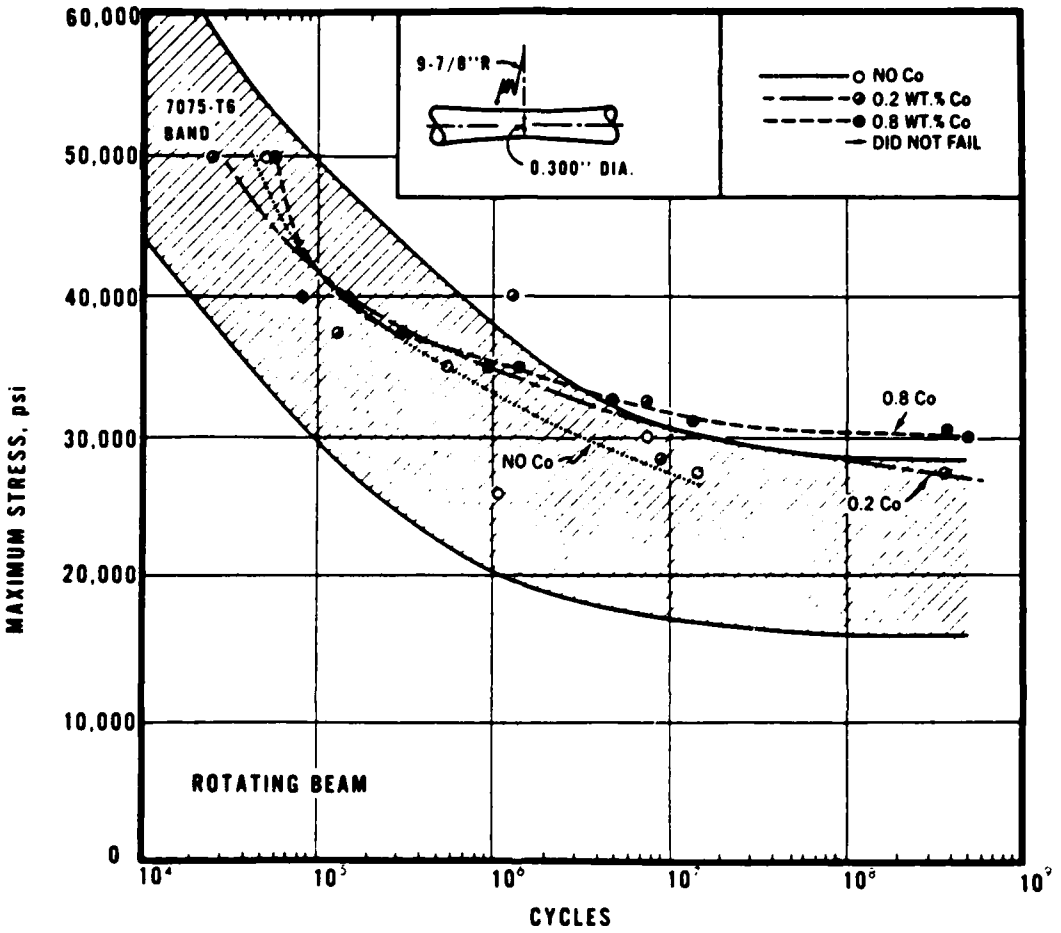

Fig. 17 A comparison of the fatigue behavior of P/M Al-6.5Zn-2.3Mg-2.0Cu and I/M 7075 T6 alloys.

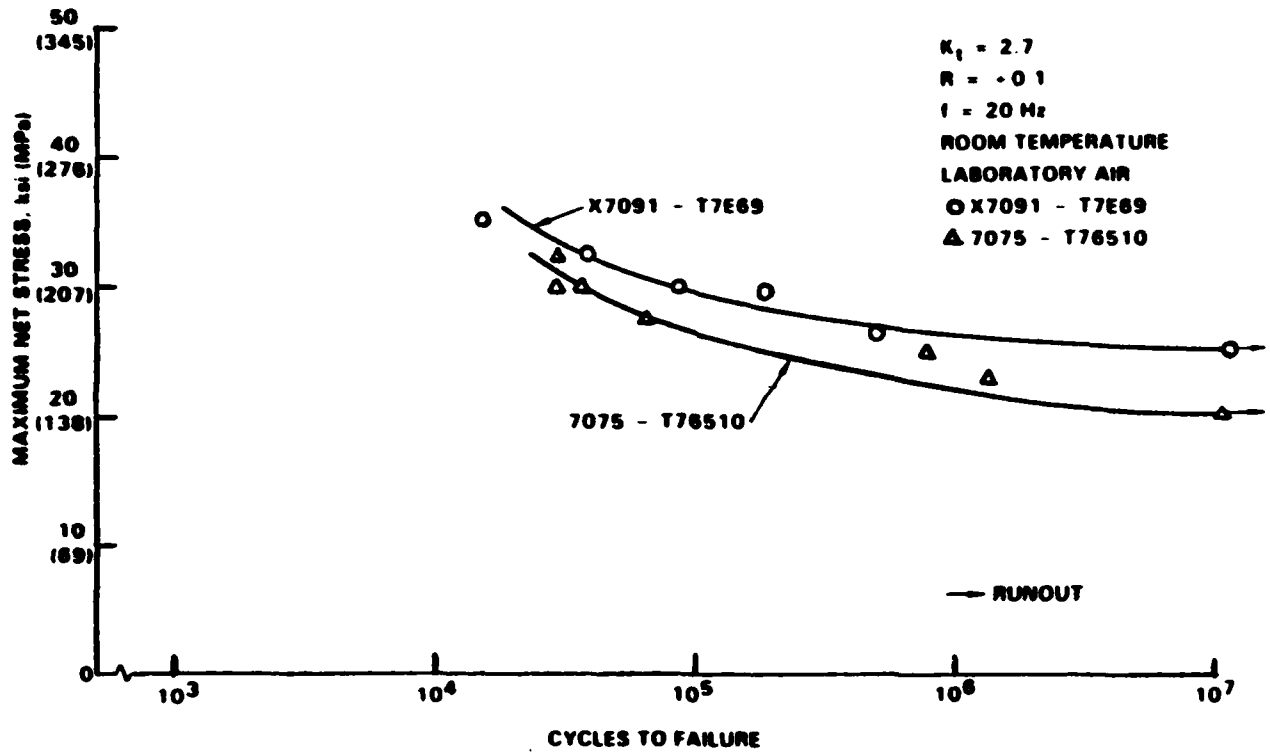

Fig. 18 A comparison of the fatigue notch sensitivity of the P/M X7091-T7E69 and the I/M 7075-T76510 alloys.

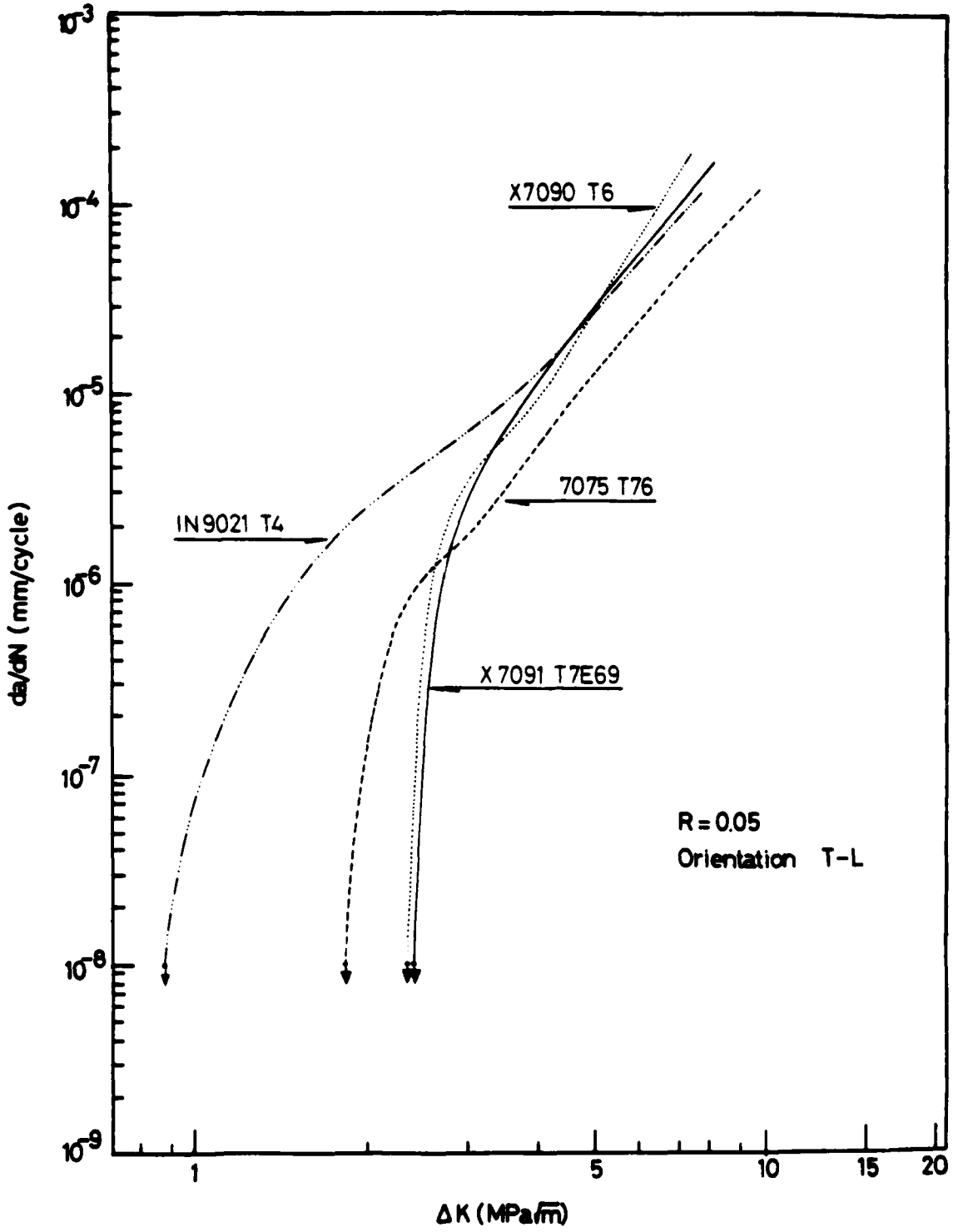

Fig. 19 A comparison of fatigue crack growth characteristics of P/M and I/M alloys.

INSTITUTE OF MATERIALS SCIENCE

The Institute of Materials Science (IMS) was established at The University of Connecticut in 1966 in order to promote academic research programs in materials science. To provide requisite research laboratories and equipment, the State of Connecticut appropriated $5,000,000, which was augmented by over $2,000,000 in federal grants. To operate the Institute, the State Legislature appropriates over $700,000 annually for faculty and staff salaries, supplies and commodities, and supporting facilities such as an electronics shop, instrument shop, a reading room, etc. This core funding has enabled IMS to attract over $2,500,000 annually in direct grants from federal agencies and industrial sponsors.

IMS fosters interdisciplinary graduate programs in Alloy Science, Biomaterials, Corrosion Science, Crystal Science, Metallurgy, and Polymer Science. These programs are directed toward training graduate students while advancing the frontiers of knowledge and meeting current and long-range needs of our state and our nation.

END

FILMED

4-84

DTIC